Stoichiometry and kinetics of mercury uptake by photosynthetic bacteria

Mariann Kis, Gábor Sipka and Péter Maróti*
Institute of Medical Physics, University of Szeged, Hungary

The publisher's version: Kis, M., Sipka, G. & Maróti, P. Photosynth Res (2017) 132: 197. https://doi.org/10.1007/s11120-017-0357-z

*Corresponding author

Rerrich Béla tér 1, Szeged 6720, Hungary

e-mail: pmaroti@sol.cc.u-szeged.hu

phone: 36-62-544-120

Keywords: Bacterial photosynthesis, intact cells, spectroscopy, Hg(II) contamination, biomediation of the environment

Abbreviations: BChl – bacteriochlorophyll, Q_A and Q_B – primary and secondary quinone acceptor, respectively, RC – reaction center protein

Abstract

Mercury adsorption on the cell surface and intracellular uptake by bacteria represent the key first step in the production and accumulation of highly toxic mercury in living organisms. In this work, the biophysical characteristics of the mercury bioaccumulation are studied in intact cells of photosynthetic bacteria by use of analytical (dithizone) assay and physiological photosynthetic markers (pigment content, fluorescence induction and membrane potential) to determine the amount of mercury ions bound to the cell surface and taken up by the cell. It is shown that the Hg(II) uptake mechanism 1) has two kinetically distinguishable components, 2) includes co-opted influx through heavy metal transporters since the slow component is inhibited by Ca^{2+} channel blockers, 3) shows complex pH-dependence demonstrating the competition of ligand binding of Hg(II) ions with H^+ ions (low pH) and high tendency of complex formation of Hg(II) with hydroxyl ions (high pH) and 4) is not a passive but an energy-dependent process as evidenced by light-activation and inhibition by protonophore. Photosynthetic bacteria can accumulate Hg(II) in amounts much (about 10^5) greater than their own masses by well defined strong and weak binding sites with equilibrium binding constants in the range of 1 $(\mu M)^{-1}$ and 1 $(mM)^{-1}$, respectively. The strong binding sites are attributed to sulfhydryl groups as the uptake is blocked by use of sulfhydryl modifying agents and their number is much (two orders of magnitude) smaller than the number of weak binding sites. Biofilms developed by some bacteria (e.g. *Rvx. gelatinosus*) increase the mercury binding capacity further by a factor of about five. Photosynthetic bacteria in the light act as sponge of Hg(II) and can be potentially used for biomonitoring and bioremediation of mercury contaminated aqueous cultures.

Introduction

After recognition of transformation of metal compounds in the environment by non-phototrophic bacteria, bacterial processing of inorganic compounds became a topic of interest in the past decades (Kane et al. 2016). Several groups have demonstrated that photosynthetic bacteria are also able to metabolize metals and metalloids and became additional possible candidates in bioprotection and bioremediation of the environment (Mehta and Gaur 2005; Singh et al. 2009; Glick 2010). Trace metals essential (manganese, iron, cobalt, copper, zinc, etc.) or non-essential (e.g. mercury) for life can be either adsorbed on the cellular surface or taken up by passive/facilitated uptake through porins/channels or by active transport through the membrane. The adsorption occurs by several chemical/functional groups (Italiano et al. 2009) that attract and sequester pollutants (Abdi and Kazemi 2015). It is nonspecific, fast and independent on the metabolism (Sloof et al. 1995; Chang et al. 1997; Bakkaloglu et al. 1998; Torres et al. 1998; Ahluwalia and Goyal 2007). On the other hand, the facilitated and active modes of uptake are slower and are closely connected to metabolic, enzymatic and energetic processes of the cell (Malik 2004; Munoz and Guieysse 2006). The transport systems are driven either by the hydrolysis of ATP (*e.g.* ATP-binding cassette (ABC) transporters (Ma et al. 2009)) or by coupling to an energetically favorable transfer of protons (*e.g.* Nramp proteins (Nevo and Nelson 2006)).

To reveal the metal-binding mechanism, the pathways of metal adsorption and uptake should be studied separately. Although there have been many studies over the last decades describing metal homeostasis in numerous bacteria and many common patterns and homologous transporters/metallochaperones across diverse phyla (Youssef et al. 2015), there is no consensus on several essential points. Some investigators have shown that metabolic activity reduces the extent of bound metal ion due to competition with protons produced by living cells (Moore and Kaplan 1994; Gabr et al. 2008), while in other cases intact cells have shown higher affinity for heavy-metal binding (Puranik and Paknikar 1999; Asztalos et al. 2010).

Among the heavy metals, mercury has a distinguished role due to its prevalence as a pollutant in aqueous systems and its very high toxicity to living organisms. Deeper understanding of Hg dynamics in anoxic environments with respect to methylation (resulting an outmost toxic form of mercury) may involve ecological and environmental context. The mercury uptake by anoxygenic phototrophs as the primary step has severe influence on the cycling of inorganic Hg and methylmercury in the food web of anoxic environments. Field and laboratory experiments have shown that phototrophs can directly interact with Hg and abet its speciation and fate (Gregoire and Poulain 2014). Once mercury accumulates in aquatic food webs, it is biomagnified from bacteria, to plankton, through macroinvertebrates, to herbivorous fish and to piscivorous (fish-eating) fish (Wiener et. al. 2003).

The mercuric ions seem to serve no biologically relevant function. Instead, they cause damage on different levels of the organism. By translocation of the mercury ions through the cell membranes, the intracellular metal-binding sites are exposed (Gourdon et al. 1990) that ultimately can result in death of sensitive organisms unless a means of detoxification is induced or already possessed (Vijayadeep and Sastry 2014). The damage is mostly due to the avidity of the mercuric ions for the sulfhydryl groups of proteins, which they block and inactivate and to high affinity for phosphate groups and active groups of ADP or ATP, and for replacement of Fe from some iron-sulfur clusters (Patra and Sharma 2000; Nabi 2014). Organic and inorganic mercurials have distinct effects on disruption of protein-iron centers: inorganic mercury was found much more efficient at removing iron from iron-dependent proteins than organic mercury compounds in *E. coli* bacteria (LaVoie et al. 2015).

Photosynthetic organisms are vulnerable to mercury exposure: in photosynthetic bacteria of *Rba. sphaeroides* 2.4.1, the half lethal dose (concentration) is two or three orders of magnitude smaller than those of any other metal ions (Giotta et al. 2006; Asztalos et al. 2010).

Mercury affects both light and dark reactions of bacterial photosynthesis and strongly inhibits the photosynthetic electron transport chain in which the reaction center (RC) protein is the most sensitive target (Asztalos et al. 2012; Kis et al. 2015). On the acceptor side, the Hg-induced inhibition is attributed to the damage of the interquinone electron transfer from Q_A to Q_B and/or to the increase of the fraction of closed RCs (Q_A^-). The donor side is much more resistant to Hg than the acceptor side. Although these data support that Hg(II) has no physiological function, it has been shown recently that Hg(II) might act in the presence of intracellular redox imbalance as sink of electrons to maintain redox homeostasis in purple bacteria (Gregoire and Poulain 2016).

Very little is known regarding the mechanism of uptake of inorganic Hg(II) by photosynthetic organisms, in part because of the inherent difficulty in measuring the intracellular mercury concentration. It has been revealed that Hg(II) uptake in anaerobic bacteria is an active transport process requiring energy and not a passive process as commonly perceived (Schaefer et al. 2011). The question can be asked whether cellular Hg uptake is specific for Hg(II), or accidental, occurring via some essential metal importer. Hg(II) uptake is highly dependent on the characteristics of the thiols that bind Hg(II) in the external medium. Some Hg(II) complexations by thiols promote the uptake and others inhibit the uptake. The evaluation of mercury binding mechanism of highly resistant marine bacteria (Deng and Wang 2012) and genetically engineered photosynthetic bacteria (Deng and Jia 2011) revealed that about 70% of Hg^{2+} was bound on the cell surface, and carboxyl groups played an important role in Hg^{2+} binding. The main resistance mechanisms are attributed either to accumulation of metal scavenging internal polypeptides or to membrane-potential dependent efflux of metals through different membrane transporters. Naturally occurring metal-binding peptides, such as metallothioneins and phytochelatins (Winklemann and Winge 1994; Sigel and Sigel, 2009), are the main metal-sequestering molecules used by cells to immobilize metal ions, offering selective, high-affinity binding sites. Several genetically engineered organisms were constructed that expressed several metal-binding peptides attached to the Hg^{2+} transport system both at the cell surface and in the intracellular medium (Bae et al. 2001). The limited uptake across the cell membrane is often the rate-limiting factor for the intracellular bioaccumulation of heavy metals.

The interest of this paper was the establishment of stoichiometry and kinetic and energetic separation of different modes of mercury uptake in the frame of a molecular model of bioaccumulation of mercury by intact photosynthetic cells. Furthermore, the Hg^{2+} uptake was measured and compared quantitatively in different photosynthetic bacteria with special regards to their planktonic or biofilm mode of lives (*Rvx. gelatinosus*). Our research is aiming at 1) filling knowledge gaps in our understanding of the interplay between Hg cycle and photosynthesis and 2) facilitating the application of photosynthetic bacteria for mercury (metal) bioremediation and further renders continuous treatment more feasible for industrial use.

Materials and Methods

Bacterial strains and growth conditions. The photosynthetic purple bacterium *Rubrivivax (Rvx.) gelatinous* (wt), *Rhodospirillum (Rsp.) rubrum* (wt) and *Rhodobacter (Rba.) sphaeroides* 2.4.1 were grown in Siström's medium (Siström 1962) in completely filled screw top vessels without oxygen (anaerobic growth). The medium was inoculated from a dense batch culture (1:100) and was illuminated by tungsten lamps that assured 13 $W \cdot m^{-2}$ irradiance on the surface of the vessel as described earlier (Asztalos et al. 2010). Planktonic cells of *Rvx. gelatinosus* were harvested at early exponential phase; biofilm cells were harvested at late stationary phase of the growth where the cells were strongly connected by biofilms. The sample was bubbled with nitrogen for 15 min before measurements to preserve the anoxic conditions. The cell

density (concentration) of the culture was estimated by counting the number of individual cells with calibrated Bürker chamber under light microscope.

Chemicals. For Hg^{2+}-ion treatment of the bacteria, the mercuric ion was added to the culture in form of $HgCl_2$ (Giotta et al. 2006). 1 mM and 10 mM $HgCl_2$ stock solutions were used which were freshly prepared before the experiment. $HgCl_2$ is highly soluble in aqueous solution under physiological conditions and stable for the duration (< 1 hour) of the treatment. The bacterial samples were kept illuminated or in the dark under anoxic condition during the mercury treatment.

For pH dependence measurements, a coctail of buffers (2-2 mM) were used: 2-(N-morpholino)-ethanesulfonic acid (MES; Sigma) between pH 5.5 and pH 6.5; 1,3-bis[tris(hydroxymethyl) methylamino]propane] (Bis-Tris propane; Sigma) between pH 6.3 and pH 9.5; Tris–HCl (Sigma) between pH 7.5 and pH 9.0; 3-(cyclohexylamino) propanesulfonic acid (CAPS; Calbiochem) above pH 9.5. The pH was adjusted by stock solutions (1-1 M) of HCl or KOH.

Ficoll 400 is a highly branched polymer formed by the copolymerization of sucrose and epichlorohydrin. It is completely non-ionic, very hydrophilic and extremely water-soluble. Separations in Ficoll normally result in better preservation of cell function and morphology. We used different concentrations of Ficoll (1-10%) to planktonic cells (Georgalis et al. 2012).

FCCP, carbonyl cyanide-4-(trifluoromethoxy)-phenylhydrazone is a widely used protonophore responsible for the collapse of the chemiosmotic membrane potential (Armitage 2001; Kelly and Thomas 2001). 20 μM was added to the bacterial culture.

Nimodipine is a potent L-type Ca^{2+} channel antagonist (Ren et al. 2001). 10-100 μM was added to the samples.

Nitrendipine: Ca^{2+} channel blocker used in 50 μM concentration here. The Ca^{2+} channel blockers had no effect on the growth of bacteria even when their concentrations were higher than those sufficient for the complete inhibition of Ca^{2+} uptake (Matsushita et al. 1988).

N-Ethylmaleimide (N-Em) is a general sulfhydryl modifying agent used in 20 mM concentration as previously (Gao and Wraight 1990). It is an organic compound derived from maleic acid and contains the imide functional group. More importantly, N-Em is an alkene that is reactive toward thiols and is able to modify cysteine residues in proteins and peptides.

Determination of Hg(II) with dithizone. Dithizone (Diphenylthiocarbazone) as chelating agent for metals was used to quantify the Hg^{2+} content of the bacterial culture. Similar method is applied to screen natural waters (lakes and rivers). The amount of Hg(II) in aqueous solution of bacteria was determined by use of indirect spectrophotometric measurements of the Hg(II)-dithizone complex that has high stability constant (Théraulaz and Thomas 1994). The dithizone was solubilized in absolute ethanol (10^{-4} M) using an ultrasonic bath. All solutions were prepared freshly before the experiment. In order to prevent oxidizing decomposition, the dithizone solution was kept in the dark at < 10°C. Reagent solutions were added as 20 v/v% dithizone solution and 80 v/v% sample in distilled water (pH 3.1). The pH of the solutions was measured by a digital pH-meter. The bacterial sample was prepared in the following way: the cells were centrifuged (8000 rpm, 5 min) and then re-suspended in 10 mM NaCl. All metals were removed from the medium otherwise they would form complex with the dithizone and disturb the mercury assay. After addition of $HgCl_2$ to the bacterial culture, the cells were centrifuged. The supernatant contained the free (unbound) Hg(II) and the sedimented cells included the bound mercury ($Hg_{bound} = Hg_{total} - Hg_{free}$). The steady-state absorption spectra were recorded by a single beam spectrophotometer (Thermo Spectronic Helios) in a 1x1 cm quartz cuvette. Mercury(II)-dithizonate has an absorption band centered around 480 nm and dithizone in acidic medium (pH 3.1) shows absorption maximum at 585 nm. The mercury concentrations were determined from the difference of the absorbances (A) measured at 480 nm (Hg(II)-dithizonate) and 585 (dithizone) nm. The $R=(A_{585}-A_{480})/A_{585}$ value measures the peak-valley

difference to the maximum absorbance, is highly sensitive to the complexation of the mercury and is calibrated by use of standard curves of $HgCl_2$ solutions carried out before each measurement (Greenberg et al. 1992). The sensitivity and working range of the assay are 0.4/(μg Hg· L^{-1}) and 2–100 μg Hg· L^{-1}, respectively.

Steady-state absorption spectroscopy. The steady-state near infrared absorption spectra of the cells were recorded during the growth at room temperature by a single beam spectrophotometer (Thermo Spectronic Helios). The baselines were corrected for light scattering.

Flash-induced absorption kinetics. The kinetics of absorption changes of the whole cells induced by Xe flash were detected by a home-constructed spectrophotometer (Maróti and Wraight 1988). The electrochromic band shift of the carotenoid pigments in the photosynthetic membrane was monitored at 530 nm with reference to 510 nm (Kis et al. 2014, 2015).

Induction of BChl fluorescence. The induction kinetics of the bacteriochlorophyll (BChl) *a* fluorescence of intact cells were measured by a home built fluorometer (Kocsis et al. 2010). The light source was a laser diode (808 nm wavelength and 2 W light power) that produced rectangular shape of illumination and matched the 800 nm absorption band of the LH2 peripheral antenna of the cells. The BChl fluorescence (centered at 900 nm) was detected in the direction perpendicular to the actinic light beam with a near infrared sensitive, large area (diameter 10 mm) and high gain Si-avalanche photodiode (APD; model 394-70-72-581; Advanced Photonix, Inc., USA) protected from the scattered light of the laser by an 850-nm high-pass filter (RG-850).

Results

Kinetics and activation energy of mercury uptake

Photosynthetic bacteria take up mercury ions in two well separated kinetic steps as revealed by direct mercury determination assay (Fig. 1). The prompt (fast) uptake is very fast and the rise time cannot be resolved under our experimental conditions. This phase may reflect the adsorption of Hg(II) ions to the cell surface groups and a passive and nonspecific diffusion through the cell membrane (leakage) driven primarily by the mercury concentration gradient. Additionally, we can observe a second and much slower kinetic phase that takes place in the minute time range and may be responsible for up to 2/3 of the total mercury uptake. Both the magnitude and the rise time of the slow phase depends on the mercury concentration (Fig. 1a). The fast phase of the uptake is [Hg] dependent, since the vertical-intercept of the graph increases with increasing [Hg]. The larger is the Hg(II) concentration outside, the smaller are the partition (amplitude) and rise time ($t_{½}$) of the slow component in mercury uptake. Upon increase of the external mercury concentration from 5 μM to 50 μM, $t_{½}$ decreases from 20 min to 3 min. The internal markers sensitive to photosynthetic activity give simultaneous signal about the invasion of Hg(II) ions into the cell and their subsequent destruction of the photosynthetic apparatus. In accordance with the slow entry of mercury ions detected by mercury assay, both the variable part of the induction of BChl fluorescence (Fig. 1b) and the electrochromic bandshift of the carotenoids in the membrane (Fig. 1c) demonstrate decreasing kinetics from the level of the untreated (0 μM Hg^{2+}) sample. The decay times of the internal photosynthetic reporters are commeasurable with the half-rise times of the slow phase of mercury uptake.

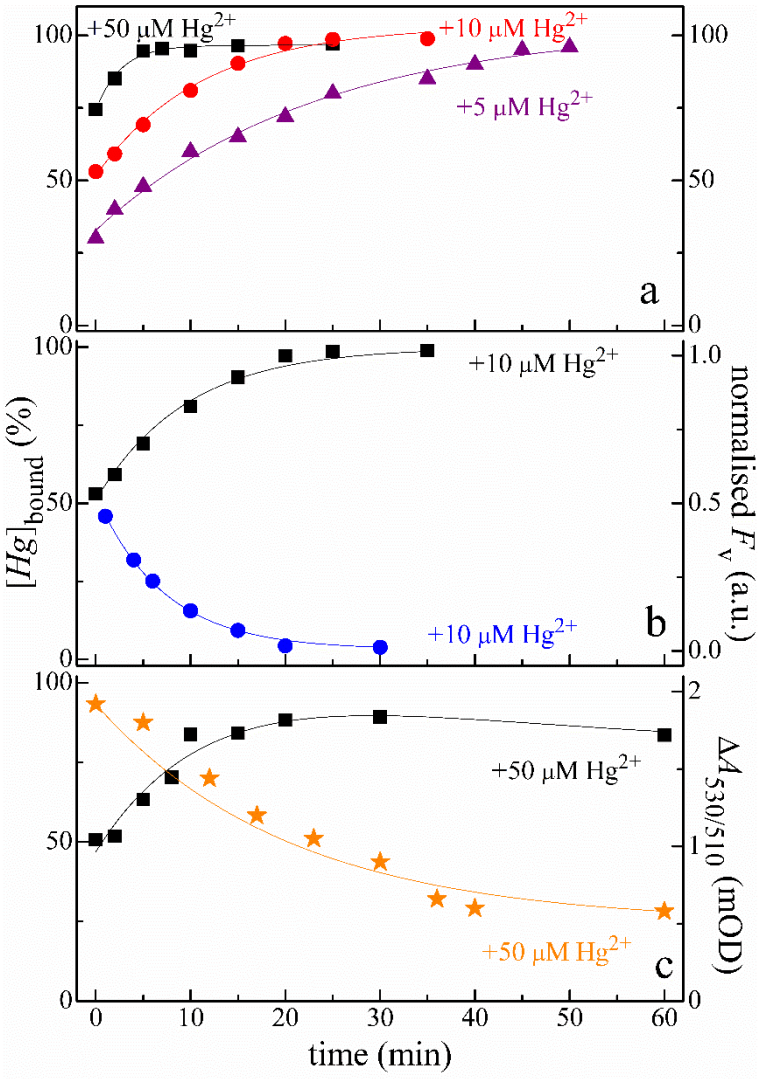

Figure 1. Fast and slow phases of Hg(II) uptake ($[Hg]_{bound}$) by photosynthetic bacterium *Rvx. gelatinosus* (panel a) and its kinetic correlation with internal photosynthetic markers of variable part (F_v) of BChl fluorescence induction (panel b) and flash-induced absorption change (ΔA_{530} vs ΔA_{510}) of the carotenoids in the photosynthetic membrane (panel c). After prompt addition of Hg(II) ions in form of $HgCl_2$, the amount of bound Hg(II) ions was determined by spectrophotometric dithizone assay at different time intervals. The cells of concentrations $1 \cdot 10^6$ (a, b) and $1 \cdot 10^8$ cell/ml (c) were kept in the light during mercury treatment. (a) The rise time ($t_{1/2}$) of the slow phase depends on the mercury concentration (■ 50 μM Hg^{2+}, $t_{1/2} = 3$ min; ● 10 μM Hg^{2+}, $t_{1/2} = 11$ min; ▲ 5 μM Hg^{2+}, $t_{1/2} = 23$ min). (b) The variable part of the induction of BChl fluorescence is referred to the untreated case (0 μM Hg^{2+}) and monitors the destruction of the photosynthetic apparatus due to 10 μM Hg^{2+}. The halftimes are 7 min (F_v, ●) and 10 min ($[Hg]_{bound}$, ■). (c) Flash-induced energetization of the membrane reflects the drop of photosynthetic activity caused by 50 μM Hg^{2+}. The halftimes are 17 min ($[Hg]_{bound}$, ■) and 20 min ($\Delta A_{530/510}$, ★).

The slow kinetic phase represents an energy consuming transport mechanism because the magnitude of the uptake increases upon energetization of the membrane evoked by illumination (Fig. 2). If the photosynthetic bacterium is exposed to continuous light excitation, the amount of bound mercury ions enhances significantly compared to that when the bacteria are kept in the dark (Fig. 2a). The photochemical gradient assures additional energy supply for

the active transport through the photosynthetic membrane. If, however, the illuminated cells are treated with FCCP, a well known protonophore, the amplitude of the mercury saturation kinetics will drop to the level corresponding to the dark situation. As FCCP makes the membrane transparent for H^+ ions, the establishment of the photochemical (proton) gradient is blocked and the membrane cannot be energized.

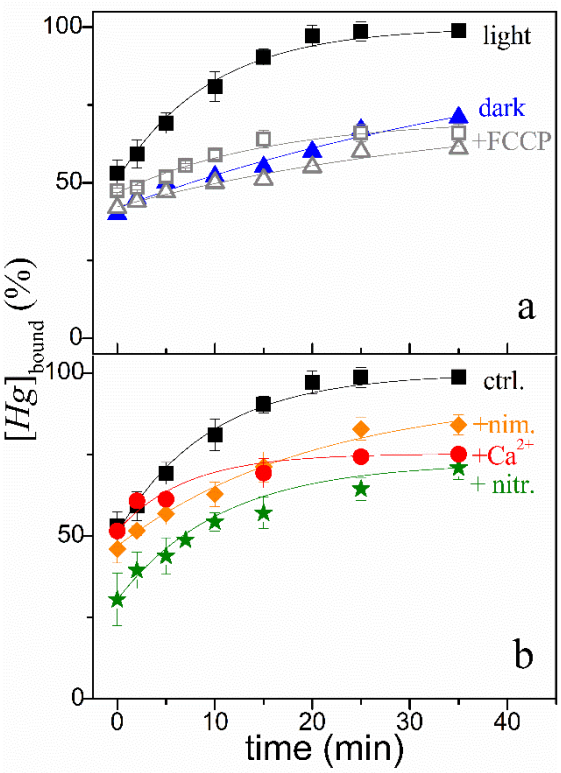

Figure 2. Correlation of the slow mercury uptake with energetization of the membrane (panel a) and Ca^{2+} transport system in the light (panel b) in *Rvx. gelatinosus*. (a) Cells treated with 10 μM Hg^{2+} bind more mercury ions in the light (■) than in the dark (▲) but not in the presence of 20 μM FCCP in the dark (Δ) and light (□). (b) Ca^{2+} channels may participate in mercury transport: the mercury uptake is diminished and deaccelerated relative to control (ctrl) upon addition of nitrendipine, a Ca^{2+} channels blocker (50 μM, ★, nitr), nimodipine, a potent L-type Ca^{2+} channel antagonist (50 μM, ◆, nitr) or Ca^{2+} ions from dissociation of $CaCl_2$ (50 μM, ●, Ca^{2+}) in the light.

Divalent cation transporters seem to contribute in side transport of mercury ions with low yield. Indeed, figure 2b shows that Ca^{2+} channels may participate in mercury transport because the uptake of Hg(II) decreases significantly upon addition of nimodipine (a potent L-type Ca^{2+} channel antagonist) and nitrendipine (a powerful Ca^{2+} channel blocker). In addition, the kinetics of slow saturation of the active uptake becomes substantially slower due to inhibition of the Ca^{2+} channels. The blockers did not affect the proton gradient and viability of the bacteria in the time- and concentration ranges of treatment which affected the active uptake of Hg (see Figs 2 and 3; Matsushita et al. 1988). Similar inhibition of the active Hg^{2+} uptake can be induced by the presence of elevated Ca^{2+} ion concentration in the suspension. These results demonstrate that a considerable portion of mercuric transport through photosynthetic membrane should occur via Ca^{2+} channels.

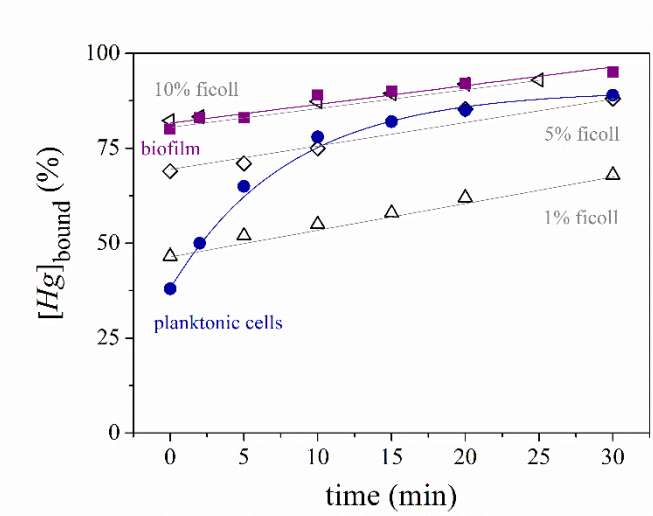

Figure 3. Comparison of the mercury uptake kinetics in planktonic cells of *Rvx. gelatinosus* (●) and cells with natural biofilm (■) or with variable concentrations of Ficoll (△ 1%, ◊ 5 % and ◁ 10 %). The cell concentrations were kept the same in all cases ($1 \cdot 10^8$ cell/mL) and 50 μM Hg^{2+} were added. The cells with polysaccharide Ficoll show similar mercury uptake kinetics as those with biofilm.

The mode of action appears to differ with the two Ca-uptake inhibitors tested, despite their target to similar Ca-voltage gated channels. Nimodipine stabilizes voltage-gated calcium channel in its inactive conformation and therefore inhibits the influx of calcium in the cells (Goyer and Cherian, 2012). Nimodipine appears to reduce Hg uptake but not affect binding to the surface. Nitrendipine, however, appears to have a more dramatic effect on Hg binding to the cell surface than uptake into the cell. Similarly, differences of modes of actions between the two Ca antagonists were observed in single cardiac transmembrane Ca channels (Hess et al. 1984).

The distinction between the diffusion and active steps of the mercury uptake is demonstrated not only kinetically but also by observed differences in activation energies. As the diffusion and active components of the mercury uptake from the bulk to the cell surface and from here to the interior of the cell are connected in series, the inverse of the observed rate (k_{obs}) of uptake is the sum of the inverses of the diffusion (k_d) and active (k_a) rates: $(k_{obs})^{-1} = (k_d)^{-1} + (k_a)^{-1}$. By measuring the observed rate, the activation energy of the rate limiting step can be determined since this step must be responsible for the overall rate. Two extreme cases were sampled in our experiments of Hg(II) binding affinity of intact cells of *Rvx. gelatinosus* (Steunou et al, 2013). In the planktonic mode of living, the diffusion step is much faster than that through the membrane ($k_d >> k_a$). In biofilm mode, however, the cell is surrounded by an extensive network of dense extracellular polymeric matrix (consisting mainly of polysaccharides) where the diffusion of mercury ions to the cell surface becomes slower than the transport through the membrane.

The increase in the amount of the uptake by diffusion and the significant deceleration of the slow phase of the mercury ions by biofilm can be modelled if the planktonic cells are connected to artificial network made of Ficoll 400 (Fig. 3). Ficoll does not have any adverse effects on viability of the bacteria and increases moreover the reproducibility of the biological sample by forming neutrally buoyant suspension (Turksen 2015). The network of polysaccharides (both of biofilm and Ficoll) decelerates the active and slow mercury uptake characteristic of planktonic bacteria so effectively that only the passive/fast phase is observable. Based on mercury saturation measurements, about 10% Ficoll is equivalent to biofilm of *Rvx. gelatinosus* i.e. their mercury uptakes show similar kinetics. It should be emphasized that the

chemical nature of the network, not the (about two-times) increased viscosity is responsible for the decreased mercury uptake.

The logarithm of the observed rate vs. the inverse of the temperature (Arrhenius plot) gives two different straight lines for the planktonic and biofilm modes of the bacterium (Fig. 4). As expected, the planktonic cells show relatively large observed rate and steep slope that corresponds to 520 meV activation energy. That energy is needed to transport the Hg(II) ions into the cell. This is a relatively large activation energy that can be covered by active metabolism of the cells in the early exponential phase of growth. While large, this energy can be achieved by the cell because it can manage this energy of activation in the bacterial RC where similarly large activation energy is required for the interquinone ($Q_A^- \rightarrow Q_B$) electron transfer (Milano et al. 2007). In biofilm mode of growth of the cell, however, the observed rate reduces substantially and the slope of the straight line becomes also small. An activation energy of 100 meV can be derived that is characteristic of the diffusion controlled processes whose small activation energy (80–200 meV) is ascribed to the temperature dependence of the viscosity. Our experiment is able to make clear distinction between the activation energies of passive (diffusion) and active transport mechanisms.

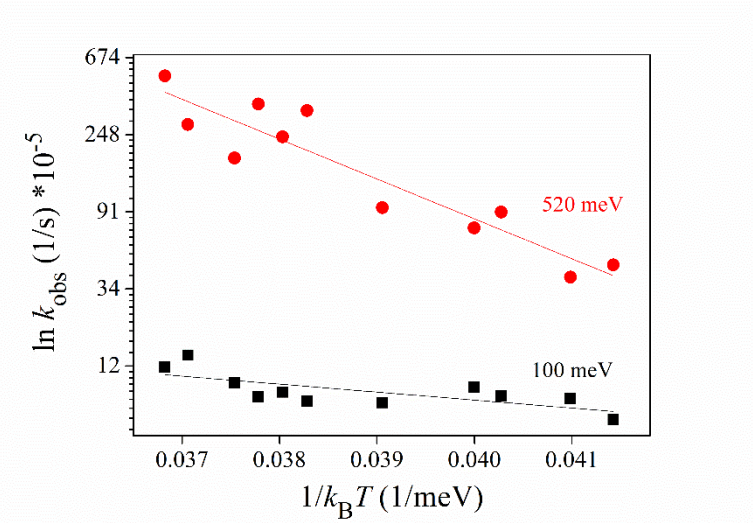

Figure 4. Determination of the activation energies of the mercury uptake of the planktonic (●) and biofilm (■) modes of the bacterium *Rvx. gelatinosus*. The logarithm of the rate limiting step (observed rate, k_{obs}) as a function of the inverse of the absolute temperature (Arrhenius-plot) is approximated by straight line whose slope is the activation energy: 520 meV (planktonic cells) and 100 meV (cells in biofilm). The conditions are the same as above.

The slow kinetic phase of Hg(II) uptake saturation depends not only on the energetization of the membrane (Fig. 2) but on the pH of the solution, as well. After corrections for the effect of pH on viability of the bacteria, the dependence of the mercury uptake on pH and time is demonstrated in the quasi 3D representation (Fig. 5). All pH profiles obtained from the plane sections parallel with the pH and time axes are highly similar: the mercury uptake has maximum at neutral pH and drops towards both the acidic and alkaline pH ranges. However, the decline is more pronounced at low pH than at high pH values. The shaded two planes represent the mercury uptake in dark and light states of the photosynthetic bacteria. The light state is characterized by light-generated protonmotive force i.e. the photosynthetic membrane is energized (~ 100 meV) compared to that of the dark state. Because the two planes do not show much (if any) differences, the light-induced energetization of the photosynthetic membrane should not affect the pH-dependence of the mercury uptake. Instead, the competition of Hg^{2+}-ions with H^+- (low pH) or OH^-- (high pH) ions will determine the shape of the pH-

dependence. The drops at pH values far from pH 7 are attributed to these competitions and not to (possible) changes of the light-generated protonmotive force.

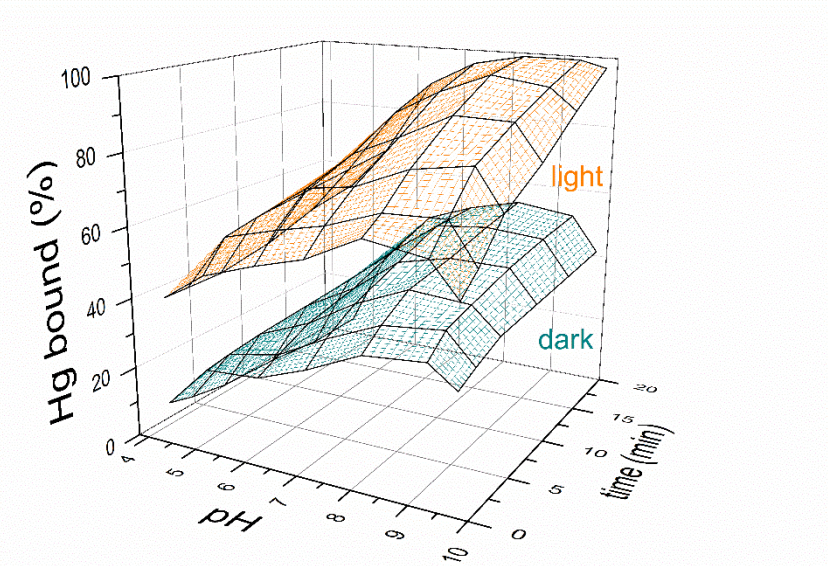

Figure 5. Quasi 3D representation of the mercury uptake of *Rvx. gelatinosus* in the dark (lower surface) and under illumination (upper surface) as funtions of the duration of the mercury treatment and pH of the culture. At all times and independently on the dark/light conditions, the mercury uptake has maximum at neutral pH and drops in the acidic and alkaline pH ranges. The view from this angle shows clearly the asymmetric pH behavior: the uptake is highly sensitive on the low (acidic) pH but less sensitive on the high (alkaline) pH. The data sets are corrected for the pH-dependence of the vitality (survival) of the bacteria and for the loss of Hg^{2+} due to HgO production in the alkaline pH range.

The formation of mercuric oxide, a toxic yellow precipitate via $HgCl_2 + 2 \cdot OH^- \rightarrow HgO + H_2O + 2 \cdot Cl^-$ should have been taken also into account as loss of $HgCl_2$ and toxic agent for bacteria in the culture at the alkaline pH range. HgO can bioaccumulate in the food chain, specifically in aquatic organisms (Greenwood and Earnshaw, 1997). As mercuric oxide appears as yellow precipitate in the culture, it increases the light scattering on a pH-dependent manner. The larger is the amount of mercuric oxide, the higher is the turbidity of the suspension. By combination of the light scattering measurement with the dithizone Hg^{2+} assay, the amount of produced HgO and loss of Hg^{2+} in the culture could be derived. At pH 10, about 20% of dissolved mercury is converted to HgO precipitate.

Multiple binding equilibria of mercury ions by cell.
As the intact cell (C) has a very large number of binding sites for interaction with small mercury ions (Hg), a relatively large mercury concentration ([Hg]~1 mM) is needed to saturate the Hg binding in a dilute suspension of cells ([C]~$1 \cdot 10^5$ cell/mL) (Fig. 6).

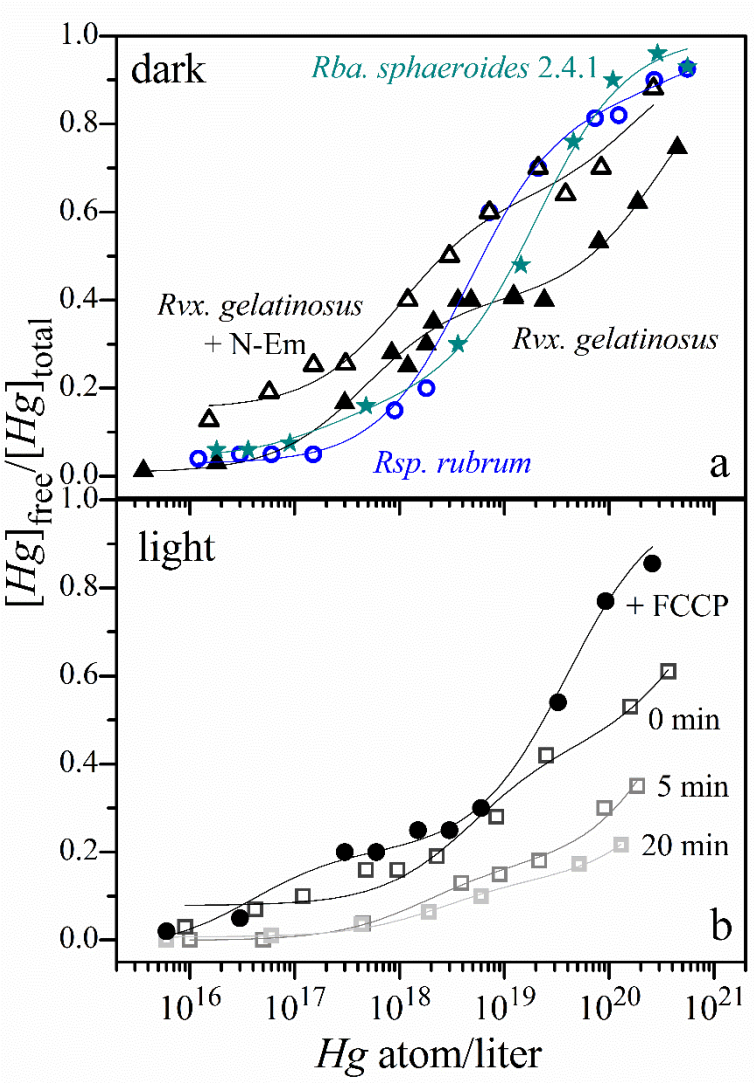

Figure 6. Saturation curves of mercury uptake for different bacterial strains under dark (a) and light (b) conditions. (a) *Rsp. rubrum* (○), *Rvx. gelatinosus* (▲), *Rvx. gelatinosus* + 20 mM N-Em (△) and *Rba. sphaeroides* (★). (b) *Rvx. gelatinosus* illuminated for 0 min (□, dark grey), 5 min (□, grey) and 20 min (□, light grey and + 20 μM FCCP (●, dark grey)). The concentration of mercury is given as the number of mercury atoms per liter. The solid lines through the measured data are the least square best fits of Eq. (4) (see Table I for the parameters).

At significantly higher cell concentrations, the cells tend to aggregate and the analysis becomes more difficult as the linearity is lost. For short exposure of the cell to ~1 mM Hg concentration, saturation can be reached without destruction of the cell. After proper analysis, the binding constants of mercury ion to the cell (K), the numbers of binding sites (n) and occupied binding sites (ν) in a single cell and cooperativity of the binding sites can be derived from the shape of the measured saturation curve. The number of occupied binding sites on the cell can be expressed as

$$\nu = \frac{[Hg]_{\text{total}} - [Hg]_{\text{free}}}{[C]}, \qquad (1)$$

where $[Hg]_{\text{total}}$ and $[Hg]_{\text{free}}$ denote the concentrations of total and free (= total–bound) Hg ions, respectively. In the simplest case of identical and independent binding sites,

$$\nu = \frac{n \cdot K \cdot [Hg]_{\text{free}}}{1 + K \cdot [Hg]_{\text{free}}}. \qquad (2)$$

If the cell possess groups of two different (weak and strong) binding sites of binding constants K_w (weak) and K_s (strong) and n_w and n_s number of sites, respectively, and the cooperativity among the binding sites may be neglected, then the occupation numbers can be added:

$$\nu = \frac{n_w \cdot K_w \cdot [Hg]_{\text{free}}}{1 + K_w \cdot [Hg]_{\text{free}}} + \frac{n_s \cdot K_s \cdot [Hg]_{\text{free}}}{1 + K_s \cdot [Hg]_{\text{free}}} \qquad (3)$$

Combining Eqs. (1) and (3), one can express the experimentally measured $[Hg]_{\text{free}}/[Hg]_{\text{total}}$ ratio as a function of the free Hg concentration:

$$\frac{[Hg]_{\text{free}}}{[Hg]_{\text{total}}} = 1 - \frac{n_w \cdot K_w \cdot [C]}{1 + K_w \cdot [Hg]_{\text{free}}} - \frac{n_s \cdot K_s \cdot [C]}{1 + K_s \cdot [Hg]_{\text{free}}} \qquad (4)$$

Table I. Number of binding sites (n) and binding constants (K) for weak and strong binding of mercury to different bacterial strains under various conditions (treatment with chemicals, illumination and time delay after mercury addition). The parameters were derived by least square fitting of the mercury saturation curves (see e.g. Fig. 6) by Eq. (4).

	Fitting parameters			
	n_s	n_w	K_s	K_w
	$\cdot 10^9$	$\cdot 10^{12}$	$(\mu M)^{-1}$	$(mM)^{-1}$
Species				
Rsp.rubrum	7.6	0.16	0.13	1
Rba.sphaeroides	0.06	0.03	2.8	30
Rvx.gelatinosus	0.4	0.4	1.25	2
Chemicals				
	Dark			
Nimodipine	0.7	0.3	0.4	2.7
n-Em	0	0.03	0	26
	Light			
Nimodipine	1	0.4	0.4	1.6
FCCP	0.03	0.07	9	13
Time				
0 min	3.5	0.9	0.12	0.8
5 min	0.6	1	0.34	1
20 min	0.7	2	0.24	0.5

As the binding constants differ greatly (by two orders of magnitude, at least), the analysis of the binding situation is not so difficult in our case. The results of decomposition of the experimentally obtained saturation curves into two components according to Eq. (4) for different bacteria strains and conditions are summarized in Table I. From the large number of binding sites, one can see that photosynthetic bacteria serve as sponge of mercury ions as they can accumulate Hg(II) in amounts much (at least 10^5 times) greater than their own masses.

If the concentration of the cells is too large ([C]>>$1\cdot10^6$ cells/mL), the actual mercury concentration will far not saturate the bacteria, therefore the parameters of Hg(II) binding cannot be obtained in that way. Instead of the analysis of the whole saturation curve, the determination of the initial value can be used to compare the mercury binding capacities of different bacteria. The limiting value is

$$\lim_{[Hg]_{total}\to 0} \frac{[Hg]_{free}}{[Hg]_{total}} = \frac{1}{1+n\cdot K\cdot[C]}, \qquad (5)$$

where n and K refer to the number of binding sites and the equilibrium binding constant of the strongest binding, respectively. The product $n\cdot K\cdot[C]$ measures the mercury binding capacity of the bacterial culture. Adjusting the same cell concentration ([C] = $1\cdot10^{13}$ cell/L) for different highly concentrated samples, their mercury binding capacities can be compared (Table II). *Rba. sphaeroides* has twice less capacity than *Rvx. gelatinosus* in planktonic mode that has five times less capacity than in biofilm mode. The increase in the latter case may be attributed to the mercury binding of the biofilm.

Table II. Comparison of the mercury binding capacities ($n\cdot K\cdot[C]$) of highly concentrated cultures of photosynthetic bacteria ([C] = $1\cdot10^{13}$ cell/L) based on measurement of the initial limiting value of the mercury saturation curves (see Eq. (5)). Notations abs and rel mean the absolute and relative values of $n\cdot K\cdot[C]$, respectively.

strain	$\lim_{[Hg]_{total}\to 0} \frac{[Hg]_{free}}{[Hg]_{total}}$	$n\cdot K\cdot[C]$	
		abs	rel
Rba. sphaeroides 2.4.1	0.18	4.5	1.0
Rvx. gelatinosus			
planktonic	0.10	9.0	2.0
biofilm	0.02	49	11

Discussion

The discussion will focus on four aspects of mercury accumulation in intact photosynthetic bacteria.

Kinetics and mechanisms of mercury binding/uptake

Based on Hg assay, we could clearly decompose the kinetics of mercury uptake into two (fast and slow) components. The fast phase includes a) biosorption of mercury ions to extracellular cell surface associated polysaccharides and proteins and b) passive diffusion through the membrane. The passive uptake is rapid, reversible, relatively nonspecific with respect to the metal species and independent of cellular metabolisms (enzymatic processes) and physical conditions such as pH and ionic strength. It is defined as an attribute of the inactive or dead microbial biomass to bind and concentrate mercury ions even from highly dilute solutions. The comparatively slow kinetic phase, however, reflects active processes and depends on the cellular metabolism as seen from decreased rate observed with protonophore (Fig. 2). The mercury(II) ions may utilize various energy-dependent transport systems including ion pumps, ion channels and carrier mediated transport.

Potentially toxic metals could be transported across the membrane via the channel (pump) of essential ions (Langston and Bebianno 1998). Calcium provides the most common divalent cationic channel and is the most likely route for entry of a number of metal pollutants including mercury. We demonstrated that Hg(II) ion influx across the bacterial membranes was

affected by Ca-channel blockers nimodipine (Hinkle et al. 1987) and nitrendipine (Barton 2005) which indicates the involvement of Ca-channels in the mercury transport process: it is associated with and competed by the transport of Ca^{2+} ions (Fig. 2). This finding is in accordance with observation of decreased Hg^{2+} accumulation by gram-negative bioreporter upon increasing divalent cation (Ca^{2+}) concentrations (Daguené et al. 2012). The authors proposed that divalent cations contributed to hamper net Hg^{2+} accumulation by decreasing outer membrane permeability and, therefore, the passive diffusion of Hg^{2+} species to the periplasmic space.

We were able to separate the passive and active modes of mercury uptake based not only on kinetics but on activation energy, as well. While the passive uptake has low activation energy (~100 meV) in accordance with our hypothesized diffusion mechanism, the active transport requires much (about 5 times) larger activation energy (~500 meV). We could model this switch between the rate limiting steps by changing the condition of cultivation for bacterium *Rvx. gelatinosus*. In the early exponential phase of growth, the cells of this strain are planktonic. The dissolved mercury is readily available to the cells therefore its rate of diffusion will not limit the kinetics of the Hg uptake. In the late stationary phase of growth, however, the cells become incorporated in biofilm and the diffusion of mercury to the cell surface through the biofilm becomes the bottle neck of the rate of Hg uptake.

The mercury uptake is pH-dependent

The pH-dependence of mercury accumulation is a diverse field of research with many particular observations and results that are difficult to treat comprehensively (Kelly et al. 2003; Le Faucheur et al. 2011; Italiano et al. 2009). Here, we observed pH-dependent bioaccumulation of mercury with the largest value at the neutral pH range and decreased substantially upon acidification and alkalization of the solution. Kelly et al. (2003) reported an opposite pH-tendency by an aquatic bacterium in a narrow ($6.3<pH<7.3$) range. Le Faucheur et al. (2011) have examined the influence of pH on Hg(II) uptake (mainly in the form of the lipophilic complex $HgCl_2$) by the green, unicellular alga, *Chlamydomonas reinhardtii* and observed that the uptake of the dichloro complex increased by a factor of 1.6 to 2 when the pH was lowered from 6.5 to 5.5. Several mechanisms were explored to explain the enhanced uptake at pH 5.5, including pH-induced changes in cell surface binding of Hg or in Hg loss rates from cells, but none of them gave completely satisfactory explanations. Their findings imply that inorganic Hg(II) in aqueous solution behaves, in terms of uptake, neither as a lipophilic complex (the uptake of which would be expected to decrease with acidification because of algal membrane packing), nor as a cationic metal (the transport of which by facilitated transport would be expected to diminish with increasing proton concentration because of metal–proton competition at the transporter binding sites). In their experiment, mercury uptake by algae seems rather to be stimulated than inhibited by proton addition.

In this work, we demonstrated an inverse relationship of the mercury uptake to the concentration of H^+ in the acidic pH range that cannot be explained by assumption of simple diffusion of neutrally charged species $HgCl_2$ to the bacterium but rather of a pH-dependent facilitated mechanism by which Hg(II) is taken up by the cells in competition with H^+ ions or by H^+/Hg^{2+} antiport. The simplest explanation is based on the competitive binding of Hg^{2+} ions to the diverse protonatable sites of the surface groups. The lower is the pH the larger is the fraction of the protonated residues (see Maróti and Wraight, 1988 for RC) and the smaller is the amount of bound mercury ions to the protonatable sites. According to our view, deprotonated forms of protonatable residues covering the acidic pH range can be made responsible for mercury immobilization (Italiano et al. 2009).

The similar pH-behavior observed at the alkaline pH range needs different explanation than Hg^{2+} competition with H^+ ions. Mercury hydroxo-complexes available to cells, seem to be

important for the accumulation on cell surface and for permeabilization of the cell membrane and can play determining role in pH-dependence of the mercury uptake. As our light scattering experiments demonstrated, hydroxyl complexes tend to precipitate in the aqueous solution with two consequences, at least. 1) More and more alkaline solution will contain less and less active mercuric(II) ion for uptake. 2) The produced toxic forms of mercuric compounds (e.g. HgO) will start to destroy the cell. These processes will contribute to the observed drop of the mercury uptake in the alkaline pH range.

The view of pH-induced changes in bacterial mercury uptake is further supported by the experimental observation that the pH-profile established by the initial equilibrium of binding/unbinding at the cell surface is not modified essentially upon energetization of the cell membrane (see Fig. 5). Only the magnitude of the mercury uptake and not the shape of the pH-dependence changed significantly, when the membrane was energetized by light excitation.

Discussing the pH-dependence of mercury uptake by photosynthetic bacteria, the suboptimal metabolic rate for different pH values should not be glossed over because the importance of metabolism on Hg uptake was shown in this work. Most enzymes typically have optimal pH range between pH 3 and 8 that leads to a very complicated pH-dependence of the bacterial metabolism. In attempt to full description of the observed pH-dependence of the mercury uptake, the possible change of the metabolic rate should be also considered.

Hill plot of mercury uptake

After introducing the degree of saturation of the binding sites ($\Theta = \nu/n$), the Hill plot can be constructed by graphing $\log\frac{\Theta}{1-\Theta}$ versus log $[Hg]_{free}$ on base of Eq. (2) (Fig. 7). This representation can demonstrate the difference between independent and cooperative binding sites at the cost of losing information for n_w and n_s, the numbers of binding sites of different affinities of the cell. On a wide range of mercury concentration, two straight lines with slopes of 1 were found indicating no cooperation of the binding sites. It is a remarkable experimental conclusion that despite of the large number of binding sites and their large affinity of mercury ions, the binding sites are independent, i.e. their binding status does not influence the binding properties of the neighbors. The binding constants of the weak and strong binding sites can be obtained from the inverse values of the interceptions of the straight lines with the horizontal line through the half saturation value ($\Theta = ½, \log\frac{\Theta}{1-\Theta} = 0$). The strong binding sites of the cell can be associated with sulfhydryl groups as the use of N-ethylmaleimide, a general sulfhydryl modifying agent, eliminates the straight line representing the sites of high mercury affinity. One could expect cooperativity among the strong binding sites but it is also unimportant as relatively few strong binding sites are available (two-three orders of magnitude less, than that of the weak binding sites, see Table I) and their interaction can be neglected.

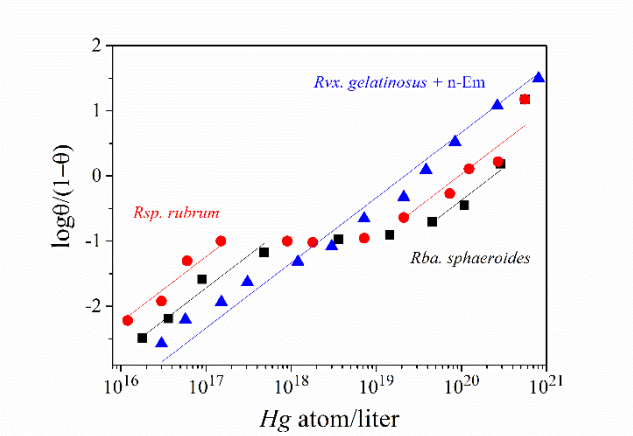

Figure 7. Hill-plots of the mercury uptake of three different strains of photosynthetic bacteria *Rsp. rubrum* (●), *Rba. sphaeroides* (■) and *Rvx. gelatinosus* (with 20 mM sulfhydryl modifying agent N-ethylmaleimide **(**n-Em**),** ▲). Note the unity slopes (no cooperativity among the binding sites) and the two (weak and strong) binding sites except of the presence of sulfhydryl modifier.

Biofilm protects the cell against mercury toxicity

Many bacteria are embedded in an extracellular polymeric substance matrix composed of polysaccharides, proteins, and nucleic acids (Flemming and Wingender, 2001). The surface-attached communities (biofilms) increase resistance to antimicrobial agents compared to the resistance of free-swimming organisms (Hentzer et al., 2001) probably due to decreased metabolic activity within the depths of a biofilm (Spoering and Lewis, 2001) and to binding and sequestration of antimicrobial agents by biofilm components, such as negatively charged phosphate, sulfate, and carboxylic acid groups (Hunt, 1986). As biofilms facilitate sorption of heavy metals, they are capable of removing heavy metal ions from bulk liquid (Liehr et al. 1994; Labrenz et al., 2000).

We observed that photosynthetic bacteria *Rvx. gelatinosus* with biofilms were more resistant to Hg^{2+} than planktonic cells (without biofilms). The effect can be attributed to the decrease of the dissolved mercury concentration because of the adsorption of the mercury species to the biofilms. The upload of the mercury pools of the cells and the biofilm are competitive processes. Another possible explanation for increased resistance to mercury in biofilms is that the negatively charged extracellular polysaccharides can effectively bind Hg^{2+} from the bulk solution (Teitzel and Parsek 2003). This view is further supported by our experiment where the natural biofilm is replaced by a similar artificial polysaccharide network produced by Ficoll. Because of the abundance of hydroxyl groups, Ficoll 400 is very hydrophilic and extremely water-soluble. Addition of Ficoll to the planktonic cells increases the passive mercury uptake to a similar level as observed in cells in biofilm mode. This finding is in contrast to Gram-negative bacterium *Escherichia coli* 055 where Najera et al. (2005) observed that the presence of the biofilm did not drastically change the relative availability of the dominant mercury species including the neutral $HgCl_2$ species dominating under our conditions.

The mercury uptake measurements have been conducted mainly with batch planktonic cultures, for which the uptake of mercury species involves diffusion across an aqueous unstirred layer to the cell surface and further through the lipid bilayer cell membrane into the cell interior. However, it is now well-established that the majority of bacteria in the environment live in attached communities or biofilms. Our model photosynthetic bacterium *Rvx. gelatinosus* is able to evolve biofilm during the growth and is expected to affect mercury availability (and its more harmful methylation) in several ways, including 1) changes in mercury speciation with steep chemical gradients within the biofilm, 2) the formation of an additional diffusive layer

surrounding cells and 3) adsorption of mercury by the biofilm. Although the photosynthetic bacterium *Rvx. gelatinosus* is unable to methylate mercury, the evolved network can colonize numerous other organisms (primarily sulphate and iron reducing bacteria and methanogens in anaerobic sediments of aquatic systems) with the capacity of methylation of Hg^{2+}. In this way, the biofilm offers stage for link between the anoxygenic phototrophs and methylators and the understanding of mercury uptake by anoxygenic phototrophs is critical from the perspective of the methylators. These organisms thrive at similar redox interfaces in the environment so there needs to be some context for what Hg uptake by phototrophs means for Hg availability to methylators and how this affects the substrate available for methylation.

Our findings shed some light on the importance of Hg availability in anoxic environments and on several potential implications for mercury cycling, including effects on elemental mercury production, mercury sedimentation, and microbial methylation of Hg(II). In a more global perspective, the present study could be part of the explanation for many environmental hazards, among others the observed connection between lake acidity and increased (methyl) mercury levels in fish (Mailman et al. 2006; Hongve et al. 2012) and the effects of primary physical-chemical factors on the harmful Hg uptake and methylation in the food webs.

Acknowledgment We are grateful to Prof. James Smart, University of Tennessee, Martin, USA for discussions and careful reading of the manuscript. Thanks to COST (CM1306), GINOP-2.3.2-15-2016-00001, OTKA-K 112688 and EFOP -3.6.2-16 for financial support.

References

Abdia O, Kazemia M. (2015) A review study of biosorption of heavy metals and comparison between different biosorbents. J. Mater. Environ. Sci. 6 (5): 1386-1399

Armitage JP (2001) Light responses in purple photosynthetic bacteria. Comprehensive Series in Photosciences, Chapter 4, 1:117-150

Asztalos E, Italiano F, Milano F, Maróti P, Trotta M (2010) Early detection of mercury contamination by fluorescence induction of photosynthetic bacteria. Photochem Photobiol Sci 9:1218-1223

Asztalos E, Sipka G, Kis M, Trotta M, Maróti P (2012) The reaction center is the sensitive target of the mercury(II) ion in intact cells of photosynthetic bacteria. Photosynthesis Research 112(2):129–140

Bae W, Mehra RK, Mulchandani A, Chen W (2001) Genetic Engineering of *Escherichia coli* for Enhanced Uptake and Bioaccumulation of Mercury. Applied and Environmental Microbiology, 67(11): 5335–5338

Barton L (2005) Structural and Functional Relationships in Prokaryotes. Springer Science & Business Media, 2005

Deng X, Jia P (2011) Construction and characterization of a photosynthetic bacterium genetically engineered for Hg^{2+} uptake. Bioresource Technology 102:3083–3088

Deng X, Wang P. (2012) Isolation of marine bacteria highly resistant to mercury and their bioaccumulation process. Bioresour Technol 121:342-7

Daguené V, McFall E, Yumvihoze E, Shurong X, Amyot, M (2012) Divalent Base Cations Hamper HgII Uptake. Environmental Science & Technology 46: 6645–6653.

Flemming H.-C, Wingender J (2001) Relevance of microbial extracellular polymeric substances (EPSs). Part I. Structural and ecological aspects. Water Sci Technol 43:1–8.

Gao J.-L, Wraight CA (1990) Sulfhydryl modifying reagents inhibit Q_A^- oxidation in reaction centers from *Rhodobacter sphaeroides* and *Capsulatus*, but not *Rhodopseudomonas viridis.* Photosynthesis Research 26(3):171-179

Georgalis Y, Philipp M, Aleksandrova R, Krüger JK (2012) Light scattering studies on Ficoll PM70 solutions reveal two distinct diffusive modes. Journal of Colloid and Interface Science 386 (1):141-147

Giotta L, Agostiano A, Italiano F, Milano F, Trotta M (2006) Heavy metal ion influence on the photosynthetic growth of *Rhodobacter sphaeroides*. Chemosphere 62:1490–1499

Glick BR (2010) Using soil bacteria to facilitate phytoremediation. Biotechnol Adv 28:367–374

Gourdon R, Bhende S, Rus E, Sofer SS (1990) Comparison of cadmium biosorption by Gram-positive and Gram-negative bacteria from activated sludge. Biotechnology Letters 12:839-842

Goyer RA, Cherian MG (2012) Toxicology of Metals: Biochemical Aspects, Springer Science & Business Media.

Greenberg AE, Clesceri LS, Eaton AD (1992) Standard Methods for the Examination of Water and Wastewater, 18th Ed., A.P.H.A., US.

Gregoire DS, Poulain AJ (2016) A physiological role for Hg(II) during phototrophic growth. Nature Geoscience 9(2):121–125

Hentzer M, Teitzel GM, Balzer GJ, Heydorn A, Molin S, Givskov M, Parsek MR (2001) Alginate overproduction affects *Pseudomonas aeruginosa* biofilm structure and function. J Bacteriol 183:5395–5401

Hess P, Lansman JB, Tsien RW (1984) Different modes of Ca channel gating behaviour favoured by dihydropyridine Ca agonists and antagonists. Nature 311: 538-544

Hinkle PM, Kinsella PA, Osterhoudt KC (1987) Cadmium Uptake and Toxicity via Voltage-sensitive Calcium Channels. J Biol Chem 262(34): 16333-16337

Hongve D, Haaland S, Riise G, Blakar I, Norton S (2012) Decline of Acid Rain Enhances Mercury Concentrations in Fish. Environ Sci Technol 46(5):2490–2491

Hunt S (1986) Diversity of biopolymer structure and its potential for ionbinding applications, pp 15–46. In H. Eccles and S. Hunt (ed.), Immobilisation of ions by bio-sorption. Ellis Horwood Ltd., West Sussex, United Kingdom.

Italiano F, Buccolieri A, Giotta L, Agostiano A, Valli L, Milano F, Trotta M (2009) Response of the carotenoidless mutant *Rhodobacter sphaeroides* growing cells to cobalt and nickel exposure. International Biodeterioration & Biodegradation 1-10.

Kane AL, Al-Shayeb B, Holec PV, Rajan S, Le Mieux NE, Heinsch SC, Psarska S, Aukema KG, Sarkar CA, Nater EA, Gralnick JA (2016) Toward Bioremediation of Methylmercury Using Silica Encapsulated Escherichia coli Harboring the mer Operon. PLOS ONE 11(1): e0147036. doi:10.1371/journal.pone.0147036

Kelly DJ, Thomas GH (2001) The tripartite ATP-independent periplasmic (TRAP) transporters of bacteria and archaea. FEMS Microbiology Reviews 25(4):405-424

Kelly CA, Rudd JW, Holoka MH (2003) Effect of pH on mercury uptake by an aquatic bacterium: implications for Hg cycling. Environ Sci Technol 37(13):2941-6

Kis M, Asztalos E, Sipka G, Maróti P (2014) Assembly of photosynthetic apparatus in *Rhodobacter sphaeroides* as revealed by functional assessments at different growth phases and in synchronized and greening cells. Photosynth Res. 122:261–273

Kis M, Sipka G, Asztalos E, Rázga Z, Maróti P (2015) Purple non-sulfur photosynthetic bacteria monitor environmental stresses. Journal of Photochemistry and Photobiology B: Biology 151:110–117

Kocsis P, Asztalos E, Gingl Z, Maróti P (2010) Kinetic bacteriochlorophyll fluorometer. Photosynth Res 105:73-82

Labrenz M, Druschel GK, Thomsen-Ebert T, Gilbert B, Welch SA, Kemner KM, Logan GA, Summons RE, De Stasio G, Bond PL, Lai B, Kelly SD, Banfield JF (2000) Formation of

sphalerite (ZnS) deposits in natural biofilms of sulfate-reducing bacteria. Science 290:1744–1747
Langston WJ, Bebianno MJ (1998) Metal Metabolism in Aquatic Environments, Springer Science & Business Media.
LaVoie SP, Mapolelo DT, Cowart DM, Polacco BJ, Johnson MK, Scott RA, Miller SM, Summers AO (2015) Organic and inorganic mercurials have distinct effects on cellular thiols, metal homeostasis, and Fe-binding proteins in *Escherichia coli*. J Biol Inorg Chem 20(8):1239–1251
Le Faucheur S, Tremblay Y, Fortin C, Campbell PGC (2011) Acidification increases mercury uptake by a freshwater alga *Chlamydomonas reinhardtii*. Environmental Chemistry 8(6): 612-622
Liehr SK, Chen H-J, Lin S-H (1994) Metals removal by algal biofilms. Water Sci Technol 30:59–68
Ma Z, Jacobsen FE, Giedroc DP (2009) Metal Transporters and Metal Sensors: How Coordination Chemistry Controls Bacterial Metal Homeostasis. Chem Rev. 109(10): 4644–4681
Mailman M, Stepnuk L, Cicek N, Bodaly RA (2006) Strategies to lower methyl mercury concentrations in hydroelectric reservoirs and lakes: A review. Science of The Total Environment 368(1):224–235
Maróti P, Wraight CA (1988) Flash-induced H^+ binding by bacterial photosynthetic reaction centers: comparison of spectrometric and conductometric methods. Biochim Biophys Acta 934:314–328
Mehta SK, Gaur JP (2005) Use of algae for removing heavy metal ions from wastewater: progress and prospects. Crit Rev Biotechnol 25:113-152
Milano F, Dorogi M, Szebényi K, Nagy L, Maróti P, Váró Gy, Giotta L, Agostiano A, Trotta M (2007) Enthalpy/entropy driven activation of the first interquinone electron transfer in bacterial photosynthetic reaction centers embedded in vesicles of physiologically important phospholipids. Bioelectrochemistry 70: 18–22
Nabi S (2014) Toxic Effects of Mercury. Springer New Delhi, p 268
Najera I, Lin CC, Kohbodi GA, Jay JA. (2005) Effect of chemical speciation on toxicity of mercury to *Escherichia coli* biofilms and planktonic cells. Environ Sci Technol 39(9):3116-20
Nevo Y, Nelson N (2006) The NRAMP family of metal-ion transporters. Biochimica et Biophysica Acta 1763: 609–620
Patra M, Sharma A (2000) Mercury toxicity in plants. The Botanical Review 66(3):379-422
Ren D, Navarro B, Xu H, Yue L, Shi Q, Clapham DE (2001) A prokaryotic voltage-gated sodium channel. Science 294(5550):2372-5
Schaefer JK, Rocks SS, Zheng W, Gu B, Liang L, Morel FMM (2011) Active transport, substrate specificity, and methylation of Hg(II) in anaerobic bacteria. Proc Natl Acad Sci USA 108:8714-8719.
Sigel H, Sigel A, eds. (2009) Metallothioneins and Related Chelators (Metal Ions in Life Sciences). Metal Ions in Life Sciences **5**. Cambridge, England: Royal Society of Chemistry. ISBN 1-84755-899-2
Singh A, Kuhad RC, Ward OP (2009) Biological remediation of soil: an overview of global market and available technologies. Advances in Applied Bioremediation. Springer, Berlin, Heidelberg.
Siström WR (1962) The kinetics of the synthesis of photopigments in *Rhodopseudomonas sphaeroides*. J Gen Microbiol 28:607-616
Spoering AL, Lewis K (2001) Biofilms and planktonic cells of Pseudomonas aeruginosa have similar resistance to killing by antimicrobials. J Bacteriol 183:6746–6751

Steunou AS, Liotenberg S, Soler M-N, Briandet R, Barbe V, Astier Ch, Ouchane S (2013) EmbRS a new two-component system that inhibits biofilm formation and saves *Rubrivivax gelatinosus* from sinking. MicrobiologyOpen 2(3):431–446

Teitzel G. Parsek M (2003) Heavy metal resistance of biofilm and planktonic *Pseudomonas aeruginosa*. Appl. Environ. Microbiol. 69: 2313-2320.

Théraulaz F, Thomas OP (1994) Complexometric Determination of Mercury(lI) in Waters by Spectrophotometry of its Dithizone Complex. Mikrochim. Acta 113:53-59

Turksen, Kursad (Ed.) (2015) Bioprinting in Regenerative Medicine. Springer International Publishing. 10.1007/978-3-319-21386-6.

Vijayadeep C, Sastry P (2014) Effect of Heavy Metal Uptake by E. coli and Bacillus sps, Journal of Bioremediation & Biodegradation 5:238

Wiener JG, Krabbenhoft DP, Heinz GH, Scheuhammer AM (2003) "Ecotoxicology of mercury," Chapter 16 *in* Hoffman DJ, Rattner BA, Burton GA, Cairns J. Handbook of Ecotoxicology, 2nd edition.: Boca Raton, Florida, CRC Press, p. 409-463.

Winkelmann G, Winge DR (1994) Metal ions in fungi. Marcel Dekker, Inc, New York, N.Y.

Youssef NH, Couger MB, McCully AL, Criado AEG, Elshahed MS (2015) Assessing the global phylum level diversity within the bacterial domain: A review. J Adv Res. 6(3): 269–282.